VERTICAL STRUCTURE OF WAVE INDUCED CURRENTS, ORBITAL VELOCITY AND TURBULENCE OBSERVED IN NATURAL VEGETATION

Hyun-Doug Yoon[1], Daniel Cox[2], Dennis Albert[3], Heather Smith[4], Nobuhito Mori[5], Philip Blackmar[6]

Vertical structures of hydrodynamics under wave conditions were investigated using live plants in a large-scale wave flume. The effect of vegetation on hydrodynamics were analyzed for regular wave cases. The interaction of waves and emergent vegetation under regular waves significantly affect wave-induced motion and turbulence intensity. Coastal vegetation motion affected the water particle kinematics so that the vertical distribution of water particle velocity showed a large deviation from linear wave theory. Also, the vegetation motion increased turbulence intensity in the middle of water column and this caused a different vertical distribution of turbulent kinetic energy compard to the control case with no vegetation. In addition to the turbulence kinetic energy level, the vegetation changed the anisotropy characteristics of turbulence, decreasing vertical turbulent component.

Keywords: nearshore processses; coastal vegetation; currents;wave-induced velocity; turbulence; large-scale laboratory experiment

Introduction

Coastal vegetation has an influence on the nearshore processes by modifying wave induced currents, orbital velocity and turbulence interacted with flexible vegetation motion. This modification affects settling velocity, sediment suspension and transport, and the exchange of momentum and/or organic materials. Previous studies have been conducted in the field or in the laboratory to understand the interaction between hydrodynamics and vegetation. Most of these studies focused on wave heights distributions (and wave height gradient) but few observations have been made on the wave-induced velocity or distribution of turbulence over the water column.

Recently, Albert et al. (2013) observed the various characteristics of bulrush (*Schoenoplectus pungens*) in coastal wetlands including plant populations, stem density, diameter, height, and flexibility. Using the same species of bulrushes, Blackmar et al. (2014) investigated wave height attenuation using small-scale artificial plants combined with numerical simulations to show how heterogeneous stands of vegetation could be modeled using a combination of drag coefficients estimated for two homogenous stands of vegetation separately. To extend the work of Albert et al. (2013) and Blackmar (2014), we provide the observation of velocity components including currents (mean velocity), orbital velocity, and turbulence since these quantities are often associated with the suspension and transport of sediment. Unlike natural beaches, the transport of sediment in vegetation is a poorly understood area, although the trapping of sediment, for example, is a valuable ecosystem service that can be provided by coastal vegetation.

In the present analysis, we present the impact of natural vegetation on the hydrodynamics observed in the large-scale laboratory experiments using live plants. This includes an analysis of the vegetation effects on the wave-induced velocity and turbulence.

Experiment

The experiments were conducted in the Large Wave Flume (104 m long, 3.6 m wide, and 4.6 m deep) at the O.H. Hinsdale Wave Research Laboratory (HWRL) at Oregon State University. Live plants (*Schoenoplectus pungens* or threesquare bulrush) were collected from the field (Tillamook, Oregon), and transplanted to twelve 8-ft long planters. Four channels were constructed with Channel A without any bulrush used for control, Channel B with the “restored” bed and Channel C and D as the natural beds. The instrumentation consisted of wire-resistance wave gages and acoustic-Doppler velocimeters

[1] Civil and Environmental Engineering, Myongji Univ., Yongin-si, Gyeonggi-do, 449-728, South Korea
[2] School of Civil and Construction Engineering, Oregon State Univ., Corvallis, OR 97333, USA
[3] Horticulture Dept., Oregon State Univ., Corvallis, OR 97333, USA
[4] Civil and Enviromental Engr., Louisiana State Univ., Baton Rouge, USA
[5] Disaster Prevention Res. Inst., Kyoto Univ., Japan
[6] School of Civil and Construction Engineering, Oregon State Univ., Corvallis, OR 97333, USA

(ADVs). Eight wave gages were installed for this study with one wave gage at the starting point of each channel and another four gages mounted on a moveable cart. Both irregular and regular waves were run with wave heights ranging $5 < H < 20$ cm and wave periods ranging $1.5 < T < 3.0$ s. There was minimal wave breaking observed during these tests. The ADVs were located at 14 vertical elevations throughout water depth for these experiments. More details were given in Yoon et al. (2011). The schematic setup and photographs of the experiment are given in Figure 1.

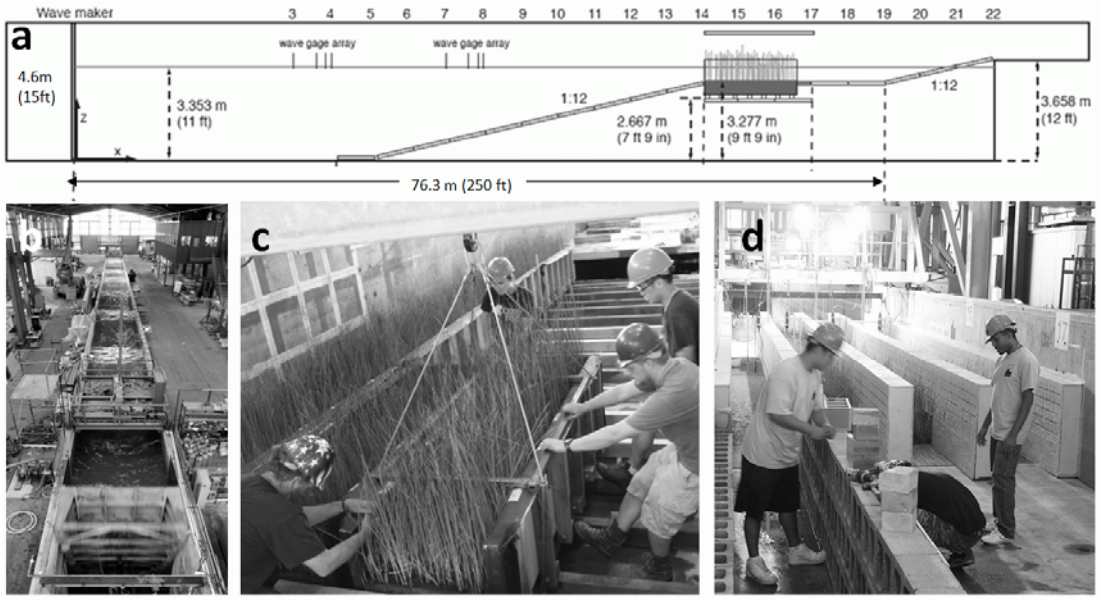

Figure 1: (a) Schematic setup of the vegetation in the flume, (b) photograph of Large Wave Flume, (c) installing bulrush beds in the flume, (d) installing false walls (Yoon et al., 2011)

Table 1 lists the experimental conditions for regular wave (Exp 2). Wave gauges were installed at x = 0 and 1.2 m. H_i is the measured wave height at x = 0 and H_{obs} is the measured wave height at x = 1.2 m. H_{est} is the estimated wave height at the location of ADV based on Kobayashi et al. (1993) as follows.

$$\frac{H(x)}{H_i} = e^{-\alpha x} \tag{1}$$

where α is the attenuation coefficient. The mean values of α were estimated 0.08 (Ch.A), 0.17 (Ch.B), 0.11 (Ch.C) and 0.28 (Ch.D). H_{est} was calculated with α for each channel with x=2.9 m and 3.0 m (ADV locations). ADV were installed at x = 2.9 m for Trial 5-21 and x = 3.0 m for Trial 22-36. For the first phase of experiment (Trial 5-21), ADV were located near water surface , ζ (elevation from the bed) = 28 cm and moved downward to the bottom. Next, the ADV were slightly moved to x = 3.0 m and the ADV measurement elevation was moved upward and the same procedure repeated. Target wave height and period were 15 cm and 1.5 s, respectively. Experiments were conducted for approximately 2 minutes for each run.

Table 1: Experimental conditions for regular wave case (Exp.2)

Trial	H_i (cm) Ch. A	Ch. B	Ch. C	Ch.D	H_{obs} (cm) Ch. A	Ch. B	Ch. C	Ch. D	H_{est} (cm) Ch. A	Ch. B	Ch. C	Ch. D	ζ (cm)
5	9.19	9.51	9.38	11.26	8.31	7.75	8.18	7.85	7.14	5.70	6.65	4.58	28
6	9.33	9.73	9.28	10.75	8.55	7.92	8.14	7.66	7.50	5.82	6.68	4.61	26
7	8.99	9.66	9.40	10.86	8.29	7.90	8.20	7.78	7.34	5.83	6.67	4.72	24
8	7.91	9.01	9.77	12.28	7.15	7.43	8.56	8.84	6.16	5.56	7.02	5.40	22
9	8.60	9.27	9.61	11.87	7.82	7.61	8.37	8.58	6.79	5.67	6.81	5.27	20
10	9.27	9.74	9.37	10.81	8.59	7.96	8.21	7.83	7.66	5.88	6.74	4.82	18
11	9.34	9.78	9.28	10.59	8.60	7.94	8.15	7.63	7.60	5.80	6.69	4.66	16
12	8.37	9.39	9.65	11.47	7.60	7.54	8.41	8.23	6.58	5.43	6.85	5.00	14
13	8.03	9.19	9.79	12.05	7.30	7.43	8.53	8.60	6.33	5.40	6.94	5.19	12
14	8.09	9.14	9.79	12.09	7.33	7.45	8.52	8.63	6.32	5.47	6.93	5.21	10
15	8.99	9.47	9.53	11.13	8.22	7.75	8.30	8.10	7.20	5.74	6.74	5.02	8
16	9.34	9.80	9.44	10.84	8.52	7.96	8.15	7.64	7.42	5.83	6.55	4.52	6
18	9.08	9.71	9.48	10.96	8.24	7.78	8.18	7.76	7.12	5.58	6.56	4.63	4
19	8.31	9.39	9.77	11.71	7.47	7.54	8.47	8.35	6.37	5.41	6.84	5.03	2
21	9.09	9.61	9.51	11.03	7.95	7.62	8.52	7.99	6.50	5.38	7.22	4.93	0
22	8.10	9.15	9.81	12.14	6.98	7.31	8.73	8.90	5.65	5.32	7.39	5.74	0
23	8.69	9.33	9.71	11.73	7.51	7.61	8.55	8.68	6.10	5.71	7.14	5.67	2
24	9.43	9.90	9.56	10.70	8.17	8.37	8.88	8.45	6.67	6.59	8.00	6.05	4
25	8.49	9.45	9.85	11.57	7.29	7.88	8.92	9.02	5.88	6.10	7.76	6.35	6
26	8.38	9.34	9.92	12.01	7.15	7.69	8.92	9.18	5.70	5.85	7.68	6.27	8
27	8.55	9.38	9.83	11.86	7.31	7.70	8.87	8.94	5.86	5.82	7.66	6.00	10
28	8.97	9.63	9.86	11.65	7.71	7.84	8.81	8.70	6.22	5.86	7.50	5.75	12
29	9.58	9.93	9.46	10.68	8.25	8.35	8.51	7.95	6.68	6.54	7.34	5.24	14
30	9.83	10.0	9.30	10.34	8.69	8.32	8.35	7.65	7.30	6.37	7.16	4.98	16
31	8.72	9.72	9.82	11.28	7.48	7.93	8.76	8.26	6.03	5.95	7.44	5.32	18
32	8.43	9.52	9.93	11.84	7.23	7.82	8.84	8.70	5.81	5.91	7.51	5.63	20
33	8.87	9.53	9.68	11.68	7.67	7.91	8.62	8.57	6.24	6.08	7.31	5.53	22
34	9.84	9.96	9.45	10.83	8.56	8.34	8.42	7.90	7.02	6.50	7.16	5.06	24
35	10.1	10.0	9.26	10.50	8.71	8.39	8.28	7.70	7.04	6.52	7.07	4.96	26
36	9.37	9.81	9.47	10.86	8.14	8.05	8.51	7.91	6.66	6.08	7.31	5.05	28

Velocity Data Reduction

Bulrush motions generate spike noises which cause unreliable estimates of the ADV data. Spike noises and turbulence in the velocity data look similar each other, therefore it is important to identify noise before estimating turbulence components from the velocity data. To detect spike noises, a signal-to-ratio (SNR) threshold and the 3D phase-space threshold method by Mori et al. (2007) were used for the velocity data. A SNR threshold of 10 dB was used first to identify spike noise, and then the 3D phase-space threshold method was used for the data which were not identified by the SNR threshold. If any component of *u*, *v*, or *w* was identified as a spike noise, all 3 components of velocity were identified as a spike noise. After spiked noises were identified, an interpolation between valid data was used to replace them.

Figure 2 shows the ensemble-averaged cross-shore velocity (*u*) from ADV. The velocity data were ensemble-averaged for 70s < t < 100s. For 30s duration, 19~21 waves were detected and were averaged to provide the ensemble-averaged velocity. Because of the bulrush motions affect the quality of ADV measurements, bad signals were shown even though the data were carefully filtered with SNR and despiking algorithm. To exclude these bad signal, waves exceeding the threshold of m+3σ where m = mean of the whole time series and σ =standard deviation of the whole time series were identified as outlier and excluded from the calculation to provide robust statistics. The excluded waves are only a small portion of the whole waves (less than 2% of total waves), so this does not affect the results significantly.

The measured instantaneous velocity (*u*) was considered to consist of mean current ($\overline{u}$), an organized wave-induced motion or ensemble-averaged motion ($\tilde{u}$), and a turbulent component (u') as

$$u = \overline{u} + \tilde{u} + u' \tag{2}$$

Also, the time-averaged turbulent kinetic energy (TKE) per unit mass is defined as

$$\bar{k} = \frac{1}{2}(\overline{u'^2} + \overline{v'^2} + \overline{w'^2}) \tag{3}$$

where the overbar refers to the turbulent intensity averaged over the entire time series of the run.

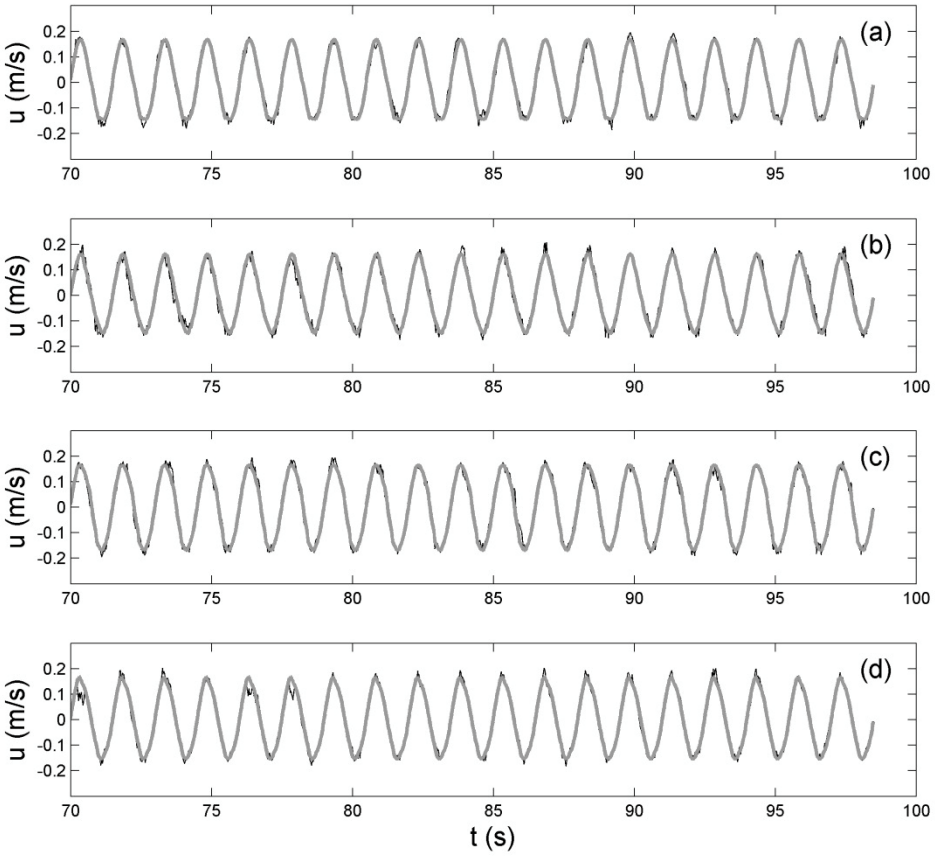

Figure 2: Example of time series of horizontal components of raw velocity (black) and ensemble averaged velocity (grey) of Trial 5 of Exp 2. Panels (a), (b), (c) and (d) represent Channel A, B, C and D.

Results

The vertical distribution of wave-induced cross-shore velocity was estimated compared to linear wave theory. The maximum and minimum of *u* from linear wave theory was calculated as follows.

$$u_{lwt}\big|_{\max,\min} = \pm\frac{H}{2}\sigma\frac{\cosh k(h+z)}{\sinh kh} \tag{4}$$

where, *H*=estimated wave height at the location of ADV based on Kobayashi et al (1993).

Figure 3 shows the wave-induced velocity of regular waves. For Channel A (no vegetation channel), the measured velocity follows the linear wave theory well over entire water depth, showing RMSE (Root-mean-square error) is within 8% of the $u_{\max,\min}$. For Channel B, C and D, the RMSE was increased by a factor of 2-3. Interestingly RMSE for $u_{\max}$ was larger than $u_{\min}$ by a factor of 2 for the

vegetated channels (Channel B, C and D) whereas there is little difference of RMSE between $u_{\max}$ and $u_{\min}$ for Channel A (no vegetation). The particle velocity was significantly affected by bulrushes when the waves moves onshore (positive u direction) rather than offshore (negative u direction).

Figure 4 shows the vertical distribution of $\overline{k}$. For the case of Channel A (no vegetation channel), the vertical distribution shows a slightly increased quantities at the both ends (i.e., near water surface and bottom). However, for the case of Channel B, C, and D (vegetation channels), turbulence were large in the middle of water column. Because of these bulrush motions, depth-averaged $\overline{k}$ for Channel B, C, and D are larger than Channel A by a factor of 2-3 (Table 3).

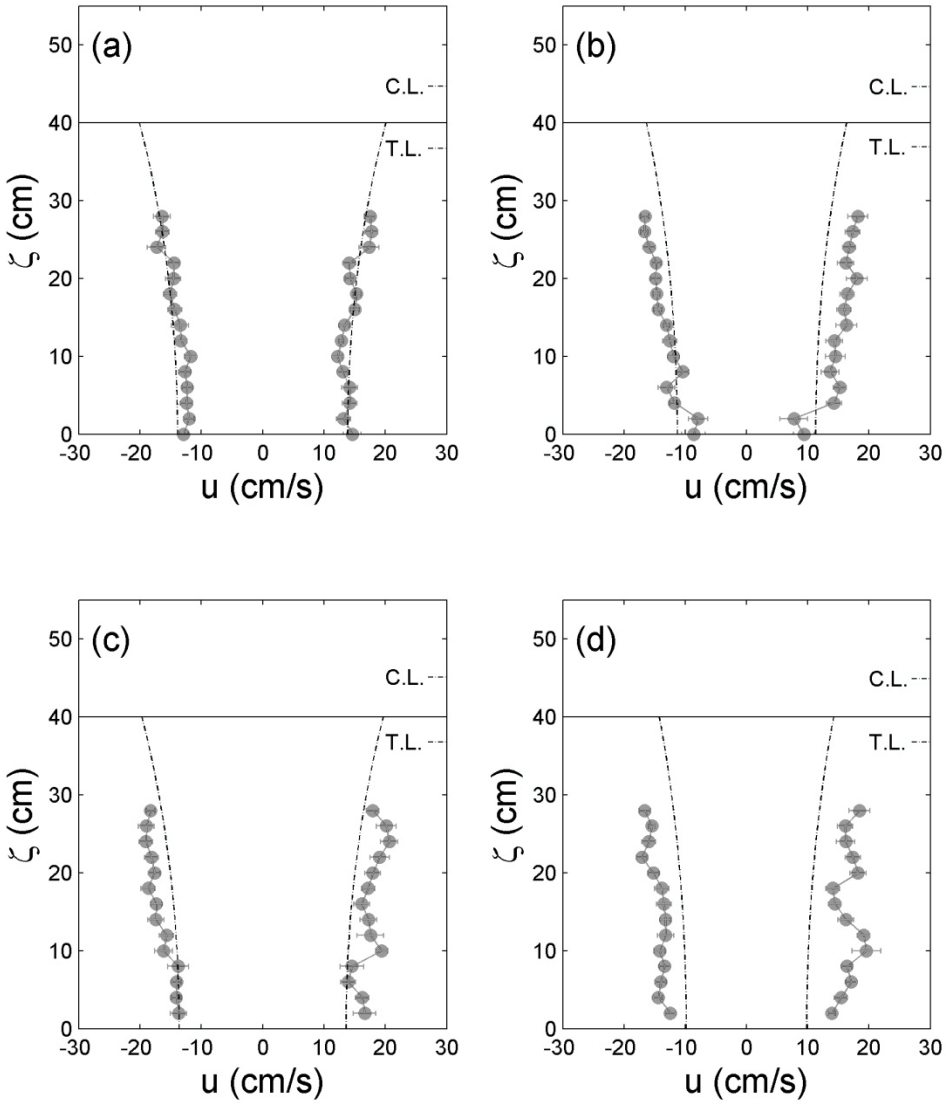

Figure 3: Vertical distribution of Umax and Umin for Exp 2. Red dots represent mean of Umax and Umin for regular waves and horizontal bars represent standard deviation of Umax and Umin. Dashdot lines represent Umax and Umin from linear wave theory. Horizontal solid lines indicate still water level. Crest level (C.L.) and Trough level (T.L) are also shown. Panels (a), (b), (c) and (d) represent Channel A, B, C and D.

Table 2: shows the RMSE between measured umax and ulwt.

	Ch.A	Ch.B	Ch.C	Ch.D
Umax	1.11	3.69	3.17	6.27
Umin	1.28	2.21	2.36	3.98

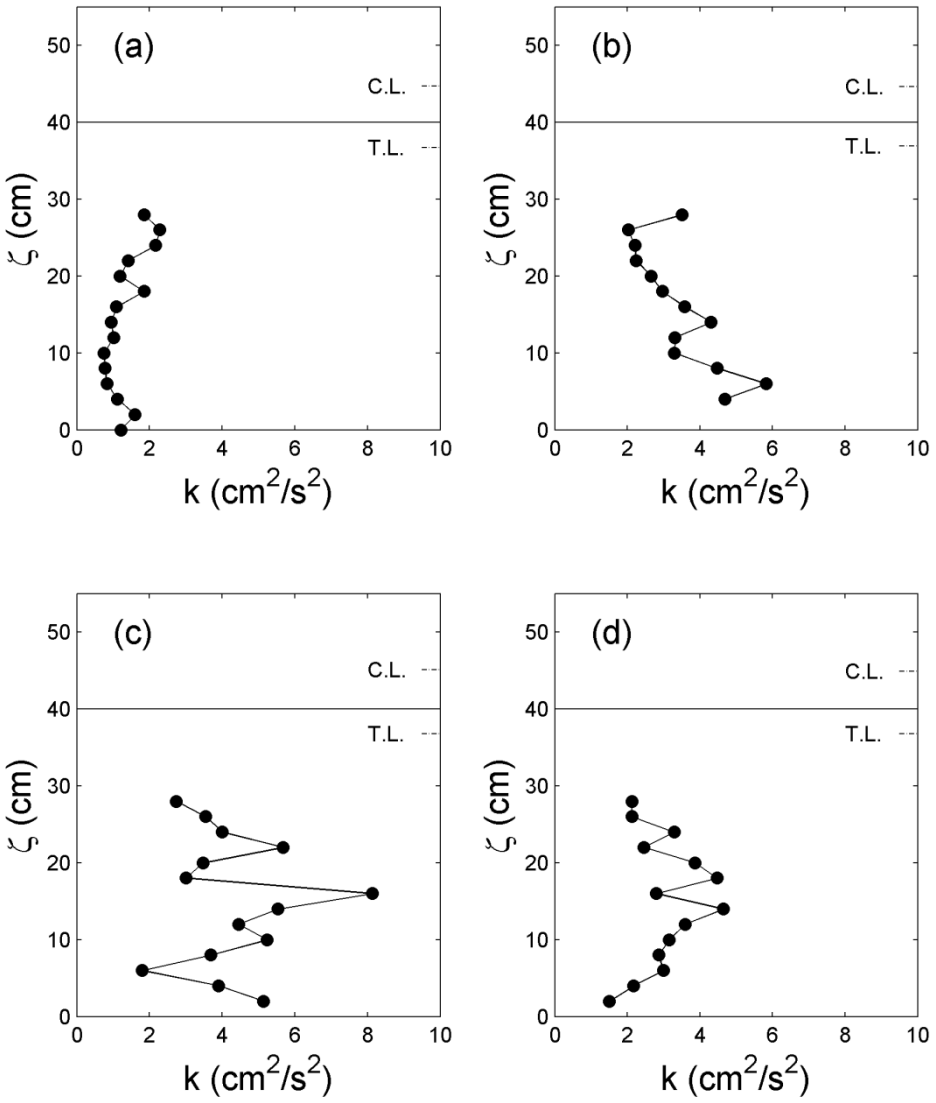

Figure 4: Vertical distribution of time-averaged turbulent kinetic energy per unit mass ($\overline{k}$) for Exp 2. Horizontal solid lines indicate still water level. Crest level (C.L.) and Trough level (T.L) are also shown. Panels (a), (b), (c) and (d) represent Channel A, B, C and D.

Table 3: Depth-averaged turbulent kinetic energy per unit mass

	Ch.A	Ch.B	Ch.C	Ch.D
Depth-averaged turbulent kinetic energy per unit mass (cm^2/s^2)	1.34	3.47	4.31	3.00

Figure 5 shows the vertical distribution of $\overline{u'^2}$, $\overline{v'^2}$ and $\overline{w'^2}$. For the case of Channel A (no vegetation channel), $\overline{u'^2}$: $\overline{v'^2}$: $\overline{w'^2}$ =0.64:0.15:0.20. For the case of Channel B, C, and D (vegetation channels), $\overline{w'^2}$ component was rapidly decreased so that $\overline{u'^2}$: $\overline{v'^2}$: $\overline{w'^2}$ = 0.50, 0.44, 0.06 for Channel B; 0.51, 0.41, 0.08 for Channel C; and 0.55, 0.37, 0.08 for Channel D, respectively. Also, the vertical distribution of $\overline{w'^2}$ was vertically uniform for the vegetated channels. Coastal vegetation motions significantly affect the anisotropy characteristics of turbulence as well as turbulent kinetic energy level, decreasing vertical turbulent component.

Conclusions

This study provides a preliminary analysis of coastal vegetation on hydrodynamics using live plants in the large-scale wave flume experiment. The interaction of waves and emergent vegetation under regular waves significantly affect wave-induced motion and turbulence intensity. Coastal vegetation motion affect water particle kinematics so that the vertical distribution of water particle velocity shows large deviation from linear wave theory. Also, vegetation motion increased turbulence intensity in the middle of water column and this caused a different vertical distribution of turbulent kinetic energy. In addition to the turbulence kinetic energy level, vegetation motion changed the anisotropy characteristics of turbulence, decreasing vertical turbulent component.

Acknowledgments

This research was supported by the National Science Foundation under Grant No. CMMI-0828549. The general support of the staff and students at the O.H. Hinsdale Wave Research Laboratory in conducting the experiment is gratefully acknowledged. Hyun-Doug Yoon was supported by Basic Science Research Program through the National Research Foundation of Korea (NRF) funded by the Ministry of Science, ICT & Future Planning (2014R1A1A1008095).

REFERENCES

Albert , D. A., D. T. Cox, T. Lemein and H.-D Yoon, 2013, Characterization of Schoenoplectus pungens in a Great Lakes Coastal Wetland and a Pacific Northwestern Estuary, *Wetlands*, doi 10.1007/s13157-013-0402-4.

Blackmar, P., D. T. Cox, and W.-C Wu, 2014, Laboratory observations and numerical simulations of wave height attenuation in heterogeneous vegetation, *Journal of Waterway, Ports, Coastal and Ocean Engr.,* Am. Soc. Civil. Eng., 140(1), 56–65.

Kobayashi, N., Raichle, A.W., and Asano, T., 1993, Wave attenuation by vegetation, *J. Wtrwy., Port, Coast., and Oc. Engrg.,* ASCE, 119 (1), 30–48.

Mori, N., T. Suzuki, and S. Kakuno. 2007. Noise of acoustic Doppler velocimeter data in bubbly flows, *J. of Engrg Mech., 133*, 122-125

Yoon. H.-D, D. T. Cox, D. A. Albert, N. Mori, H. Smith and J. Zarnetske, 2011, Ecological Modeling of emergent vegetation for sustaining wetlands in high wave energy coastal environments. *Proceedings of Coastal Structures*, Yokohama

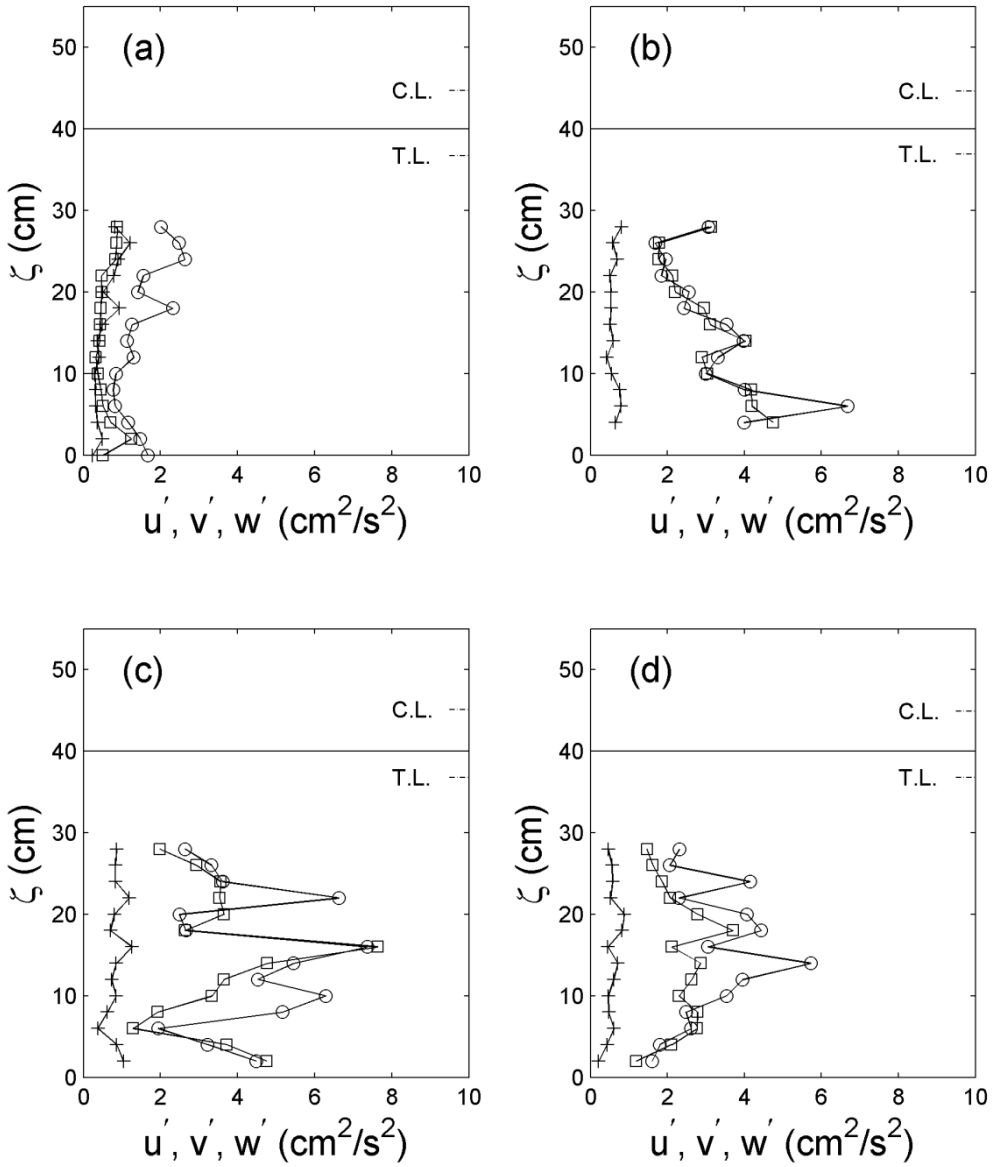

Figure 5: Vertical distribution of time-averaged cross-shore(u'^2, circle), alongshore(v'^2, square), and vertical(w'^2, plus) component of turbulence for Exp 2. Horizontal solid lines indicate still water level. Crest level (C.L.) and Trough level (T.L) are also shown. Panels (a), (b), (c) and (d) represent Channel A, B, C and D.